AD-A062 377 ARNOLD ENGINEERING DEVELOPMENT CENTER ARNOLD AFS TN F/G 22/2
EFFECTS OF VERTICAL TAIL FLEXIBILITY ON THE AERODYNAMIC CHARACT--ETC(U)
AUG 78 J A BLACK

UNCLASSIFIED AEDC-TSR-78-P29 NL

1 OF 1
ADA
062377

END
DATE
FILMED
3 -79
DDC

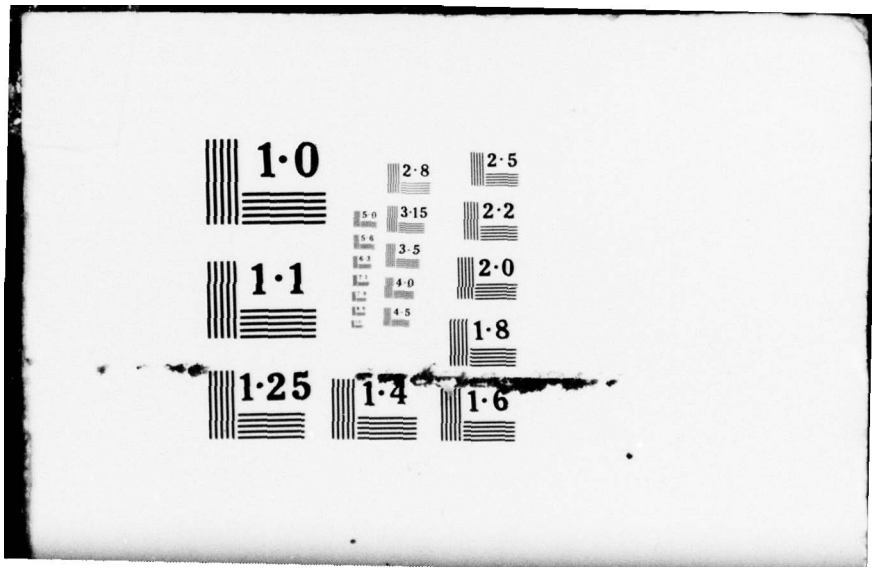
1·0
1·1
1·25
1·4
1·6
1·8
2·0
2·2
2·5
2·8
3·15
3·5
4·0
4·5
5·0
5·6

AEDC-TSR-78-P29

August 29, 1978

LEVEL II

(2)

SC

EFFECTS OF VERTICAL TAIL FLEXIBILITY ON THE AERODYNAMIC CHARACTERISTICS OF A 0.03-SCALE NASA SPACE SHUTTLE ORBITER AT MACH NUMBERS FROM 0.90 TO 1.55

J. A. Black
ARO, Inc., AEDC Division
A Sverdrup Corporation Company
Propulsion Wind Tunnel Facility
Arnold Air Force Station, Tennessee

Period Covered: July 11-15, 1978

Approved for public release; distribution unlimited.

Reviewed By:

James M. McGee

JAMES M. McGEE, 2d Lt, USAF
Test Director, PWT Division
Directorate of Test Operations

Approved for Publication:

FOR THE COMMANDER

Alan L. Devereaux

ALAN L. DEVEREAUX
Colonel, USAF
Deputy for Operations

Prepared for: Johnson Space Center
EX 33
Houston, Texas 77058

ARNOLD ENGINEERING DEVELOPMENT CENTER
AIR FORCE SYSTEMS COMMAND
ARNOLD AIR FORCE STATION, TENNESSEE

UNCLASSIFIED

(9) Final rept.,

REPORT DOCUMENTATION PAGE		READ INSTRUCTIONS BEFORE COMPLETING FORM
(14) 1. REPORT NUMBER AEDC-TSR-78-P29	2. GOVT ACCESSION NO.	3. RECIPIENT'S CATALOG NUMBER
(6) 4. TITLE (and Subtitle) Effects of Vertical Tail Flexibility on the Aerodynamic Characteristics of a 0.03-Scale NASA Space Shuttle Orbiter at Mach Numbers from 0.90 to 1.55		5. TYPE OF REPORT & PERIOD COVERED Final Report - July 11-15, 1978
		6. PERFORMING ORG. REPORT NUMBER
(10) 7. AUTHOR(s) J. A. Black, ARO, Inc., a Sverdrup Corporation Company		8. CONTRACT OR GRANT NUMBER(s)
9. PERFORMING ORGANIZATION NAME AND ADDRESS Arnold Engineering Development Center Air Force Systems Command Arnold Air Force Station, TN 37389		10. PROGRAM ELEMENT, PROJECT, TASK AREA & WORK UNIT NUMBERS Program Element 921E01
11. CONTROLLING OFFICE NAME AND ADDRESS		12. REPORT DATE (11) 29 August 1978
		13. NUMBER OF PAGES 26
14. MONITORING AGENCY NAME & ADDRESS (if different from Controlling Office) (12) 29p.		15. SECURITY CLASS. (of this report) Unclassified
		15a. DECLASSIFICATION/DOWNGRADING SCHEDULE N/A

16. DISTRIBUTION STATEMENT (of this Report)

Approved for public release; distribution unlimited.

17. DISTRIBUTION STATEMENT (of the abstract entered in Block 20, if different from Report)

18. SUPPLEMENTARY NOTES

19. KEY WORDS (Continue on reverse side if necessary and identify by block number)

Space Shuttle Orbiter
Aerodynamic Characteristics
Flexible Vertical Tail
Dynamic Pressure Effects

20. ABSTRACT (Continue on reverse side if necessary and identify by block number)

A 0.03-scale model of the NASA Space Shuttle Orbiter utilizing a flexible and a rigid vertical tail was tested during the period July 10 to 15, 1978, in the Propulsion Wind Tunnel, Transonic (16T) at free-stream Mach numbers from 0.90 to 1.55, free-stream dynamic pressures from 300 to 700 psf, angles of attack from -2 to 12 deg and angles of sideslip from -5 to 9 deg for speedbrake deflections of 25 and 55 deg, and rudder deflections of 0 and 10 deg. The objective of the test was to determine the effects of

DD FORM 1 JAN 73 1473 EDITION OF 1 NOV 65 IS OBSOLETE

042 550

UNCLASSIFIED

78 12 13 052

20. ABSTRACT (Continued)

vertical tail flexibility on the static stability and control characteristics of the Orbiter vehicle.

AFSC
Arnold AFS Tenn

CONTENTS

ILLUSTRATIONS

TABLES

NOMENCLATURE

ALFC	Sting pitch angle, deg
AFA	Test section pitch plane flow angularity, positive up, deg
ALFORB	Orbiter angle of attack corrected for flow angularity, deg
BETORB	Orbiter sideslip angle corrected for flow angularity, deg
BFA	Test section sideslip plane flow angularity, positive from right to left when looking upstream, deg
CLN	Orbiter yawing-moment coefficient
DELSB	Speedbrake deflection, deg
DELR	Rudder deflection, deg
FY1(Fig.3)	Forward side force bridge, vertical tail balance
FY2(Fig.3)	Aft side force bridge, vertical tail balance
M_ℓ (Fig.3)	Rolling moment bridge, vertical tail balance
M_m (Fig.3)	Pitching-moment bridge, vertical tail balance
MRC (Fig.3)	Moment reference center, model station about which moments are calculated
M_∞	Free-stream Mach number
PART	Part number (a data subset containing variations of only one independent parameter)
PHI, ϕ	Model roll angle, deg
PT	Free-stream total pressure, psfa
Q	Free-stream dynamic pressure, psf
UCA	Uncertainty in axial-force coefficient
UCLL	Uncertainty in rolling-moment coefficient
UCLM	Uncertainty in pitching-moment coefficient
UCLN	Uncertainty in yawing-moment coefficient

UCN	Uncertainty in normal-force coefficient
UCY	Uncertainty in side-force coefficient
UCLLV	Uncertainty in vertical tail torsional (rolling) moment coefficient
UCLNV	Uncertainty in vertical tail bending (yawing) moment coefficient
UCYV	Uncertainty in vertical tail side-force coefficient
X_o	Orbiter longitudinal station, in.
Z_o	Orbiter waterline station, in.
Z_{orb}	Location of orbiter moment reference center relative to the tunnel centerline, positive above, ft

1.0 INTRODUCTION

The work reported herein was sponsored by, and conducted for, the Johnson Space Center, Houston, Texas, under Program Element 921E01. The work was done at the Arnold Engineering Development Center (AEDC), Air Force Systems Command (AFSC), Arnold Air Force Station, Tennessee by ARO, Inc., AEDC Division (a Sverdrup Corporation Company), contract operator of the AEDC. The test was conducted in the Propulsion Wind Tunnel Facility (PWT), Propulsion Wind Tunnel, Transonic (16T) during the period July 10 to 15, 1978 under ARO Project Number P41T-34.

The objective of the test was to determine the effects of vertical tail flexibility on the aerodynamic characteristics of a 0.03-scale model of the NASA Space Shuttle Orbiter at free-stream Mach numbers from 0.90 to 1.55, angles of attack from -2 to 12 deg, and sideslip angles from -5 to 9 deg with speed-brake deflections of 25 and 55 deg, and rudder deflections of 0 and 10 deg. The effects of static loading were determined by testing at dynamic pressure levels of 300, 500, and 700 psf at all Mach numbers. Baseline data were obtained by testing the orbiter with a rigid vertical tail at a constant dynamic pressure of 400 psf at all test Mach numbers.

The final data from the test have been transmitted to Johnson Space Center, Houston, Texas. Requests for these data should be directed to Johnson Space Center, EX 33, Houston, Texas 77058. A copy of the final data is on file on microfilm at AEDC.

2.0 APPARATUS

2.1 TEST FACILITY

The AEDC Propulsion Wind Tunnel (16T) is a variable density, continuous-flow tunnel capable of being operated at Mach numbers from 0.2 to 1.6 and stagnation pressures from 120 to 4000 psfa. The maximum attainable Mach number can vary depending upon the tunnel pressure ratio requirements with a particular test installation. The maximum stagnation pressure attainable is a function of Mach number and available electrical power. The tunnel stagnation temperature can be varied from about 80 to 160°F depending upon the available cooling water temperature. The test section is 16 ft square by 40 ft long and is enclosed by 60-deg inclined-hole

perforated walls of six-percent porosity. The general arrangement of test section with the test article installed is shown in Fig. 1. Additional information about the tunnel, its capabilities, and operating characteristics is presented in Ref. 1.

2.2 TEST ARTICLE

The model used in the test was a 0.03-scale representation of the Space Shuttle Orbiter Vehicle. Two vertical tails were utilized during the test; a rigid, steel tail which bolted directly to the orbiter balance support structure, and a flexible tail consisting of an aluminum spar with rubber molded about it to produce the desired airfoil contour. The flexible vertical tail was elastically scaled considering the materials and properties of the wind tunnel model and the flight vehicle, the location of the elastic axis, and the model test and flight dynamic pressures. Rudder/speedbrake deflection angles were obtained by deflection of the four speedbrake panels to the desired angles.

Location of the model in the test section is shown in Fig. 1, and a photograph of the model installation is shown in Fig. 2. The general arrangement of the model and its primary dimensions are presented in Fig. 3.

2.3 INSTRUMENTATION

A 2.5-in.-diam, six-component internal strain gage balance was used to measure the total forces and moments on the model. Three-component (side force, bending moment, and torsion) data were obtained on the flexible vertical tail by means of strain gage bridges applied to the aluminum spar of that tail (Fig. 3b). Hinge moments on the right hand inboard and outboard elevons were measured by single component strain gaged beams. Four base pressures and two model nose pressures were measured by individual pressure transducers located in the model. Sting pitch was measured by a synchro-transmitter and sting roll was measured by a potentiometer. Electrical signals from all instrumentation were digitized for on-line data reduction and coefficient display by the facility computer. The analog signals from all balance channels were recorded on an oscillograph recorder for monitoring dynamic loading of the balance components. Data were transmitted to an IBM-370/155 computer for use by an interactive graphics system for on-line data evaluation and comparative analysis. A typical on-line plot is shown in Fig. 4.

3.0 TEST DESCRIPTION

3.1 PROCEDURE

Data were obtained by establishing the appropriate tunnel conditions and taking steady-state data over the desired angle range. Angles of attack and sideslip were obtained by combinations of model pitch and roll. Model positioning and data acquisition were computer controlled during the data acquisition sequence. The portion of the flow angularity investigation devoted to determination of pitch plane angularity was conducted by testing the model both upright and inverted. Flow angularity in the side plane was determined from tests conducted with the model rolled both 90 deg and -90 deg. The nominal model attitude test schedules are presented in Table 1, and a summary of test conditions is presented in Tables 1, 2, and 3.

3.2 DATA REDUCTION

Model, vertical tail forces and moments, and elevon hinge moments were corrected for weight tare effects and were reduced to coefficient form in the body axis system. All forces and moments from the orbiter and vertical tail balance were nondimensionalized using the orbiter reference area and lengths, with the moments referenced to a common model station on the orbiter. Elevon hinge moments were nondimensionalized using the elevon area and chord length.

Model angle of attack and sideslip were corrected for the tunnel stream angularities, using the data shown in Fig. 5, during a post-test recomputation of the data. The pitch plane flow angularity (AFA) was found to be invariant with model vertical location in the tunnel within the location envelope indicated in Fig. 6. The pitch plane angularity corrections were applied using a polynomial curve fit of AFA as a function of M_∞. Cross-flow angularity (BFA) was found to be a function of both Mach number and vertical location in the test section. This correction was inserted as a table look-up with double linear interpolation.

The two side force bridges on the vertical tail balance were found to be sensitive to thermal effects. When post test instrumentation checks indicated significant zero shifts in the instrumentation, the data were recomputed using one-half of the indicated shift; thus minimizing the error in the data.

3.3 UNCERTAINTY OF MEASUREMENTS

Uncertainties (bands which include 95 percent of the calibration data) of the basic tunnel parameters, shown in Fig. 7, were estimated from repeat calibrations of the instrumentation and from the repeatability and uniformity of the test

section flow during tunnel calibration. Additional information concerning the uncertainties in the free-stream properties is discussed in Refs. 2 and 3. Uncertainties in the instrumentation systems were estimated from repeat calibrations of the systems against secondary standards whose uncertainties are traceable to the National Bureau of Standards calibration equipment. The instrument uncertainties are combined using the Taylor series method of error propagation described in Ref. 4 to determine the uncertainties of the reduced parameters shown in Table 4. Uncertainties in longitudinal coefficients (C_N, C_A, and CLM) are presented for angles of attack of 2, 6, and 10 deg. Uncertainties in lateral-directional coefficients (CY, CLL, and CLN) and all vertical tail coefficients are presented for sideslip angles of 2, 5, and 9 deg. Uncertainties in model angles of attack and sideslip are estimated to be ±0.14 deg and ±0.18 deg, respectively.

4.0 DATA PACKAGE PRESENTATION

A summary of test conditions is presented in Tables 1, 2, and 3 correlating the vertical tail being testing, speedbrake deflection, rudder deflection, and type of data being acquired, with test part number, Mach number, and free-stream dynamic pressure. A sample of the tabulated data summary is shown in Table 5. The nomenclature associated with the summary tabulation is given in Table 6. In addition to the printed summary and a point-by-point data tabulation, the data package contained selected model installation photographs and a microfilm copy of all the data. The data package was transmitted to NASA, Johnson Space Center, Houston, Texas.

REFERENCES

1. Test Facilities Handbook (Tenth Edition). "Propulsion Wind Tunnel Facility, Vol. 4." Arnold Engineering Development Center, May 1974.

2. Gunn, J. A. "Check Calibration of the AEDC 16-ft Transonic Tunnel." AEDC-TR-66-80 (AD633277), May 1966.

3. Jackson, F. M. "Supplemental Calibration Results for the AEDC Propulsion Wind Tunnel (16T)." AEDC-TR-70-163 (AD872475), August 1970.

4. ICRPG Handbook for Estimating the Uncertainty in Measurements Made with Liquid Propellant Rocket Engine Systems. Interagency Chemical Rocket Propulsion Group CPIA No. 180, April 30, 1969.

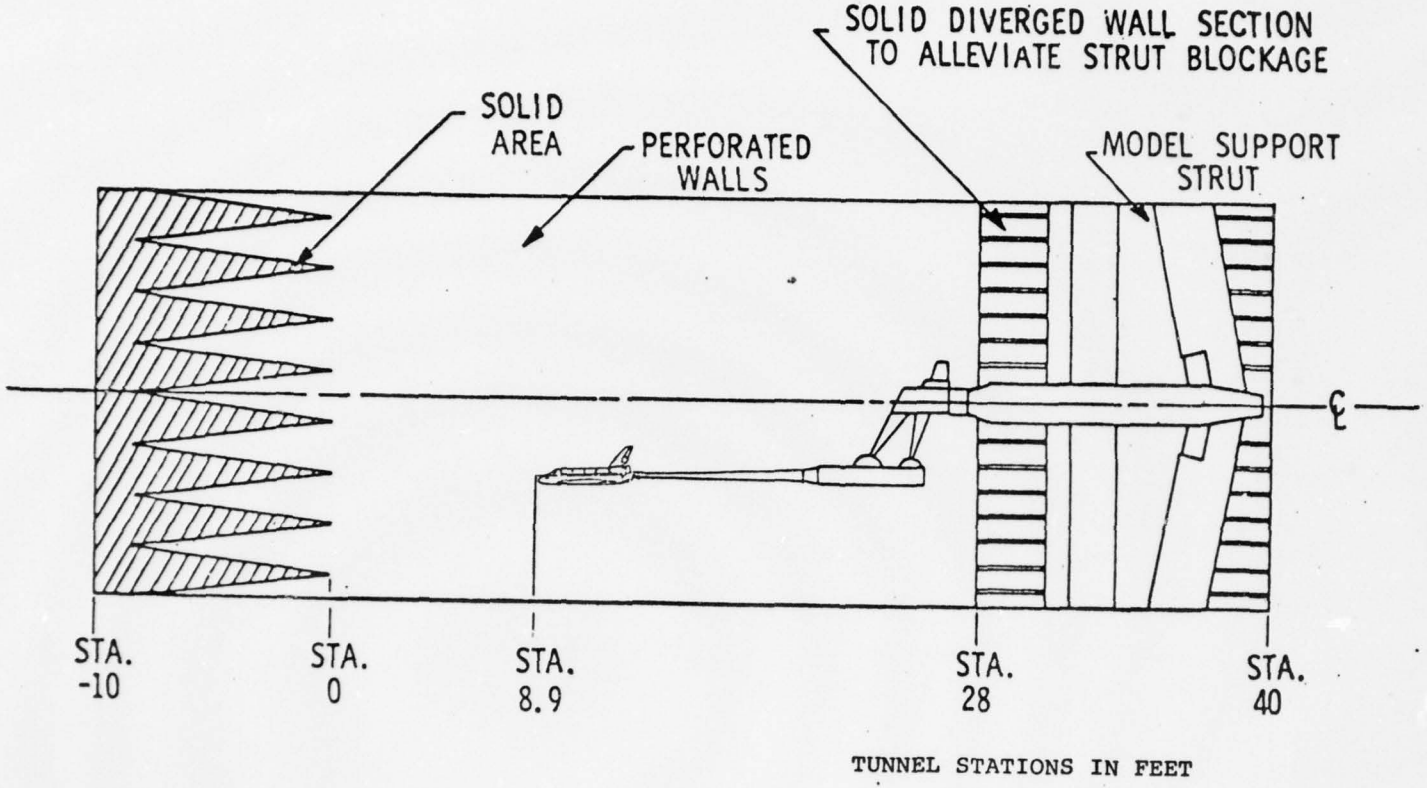

Figure 1. Location of the Test Article in the Test Section

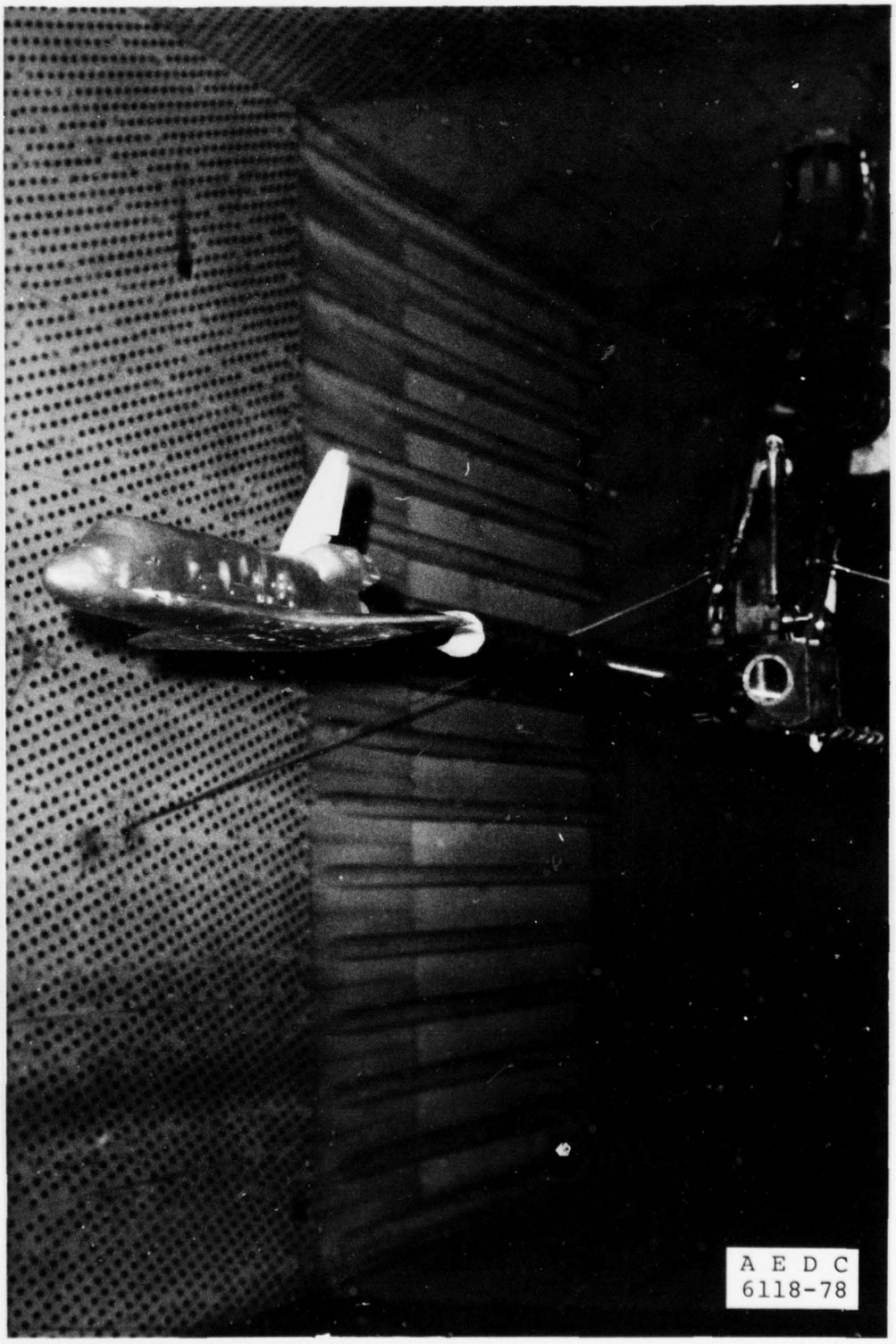

Figure 2. Test Article Installation

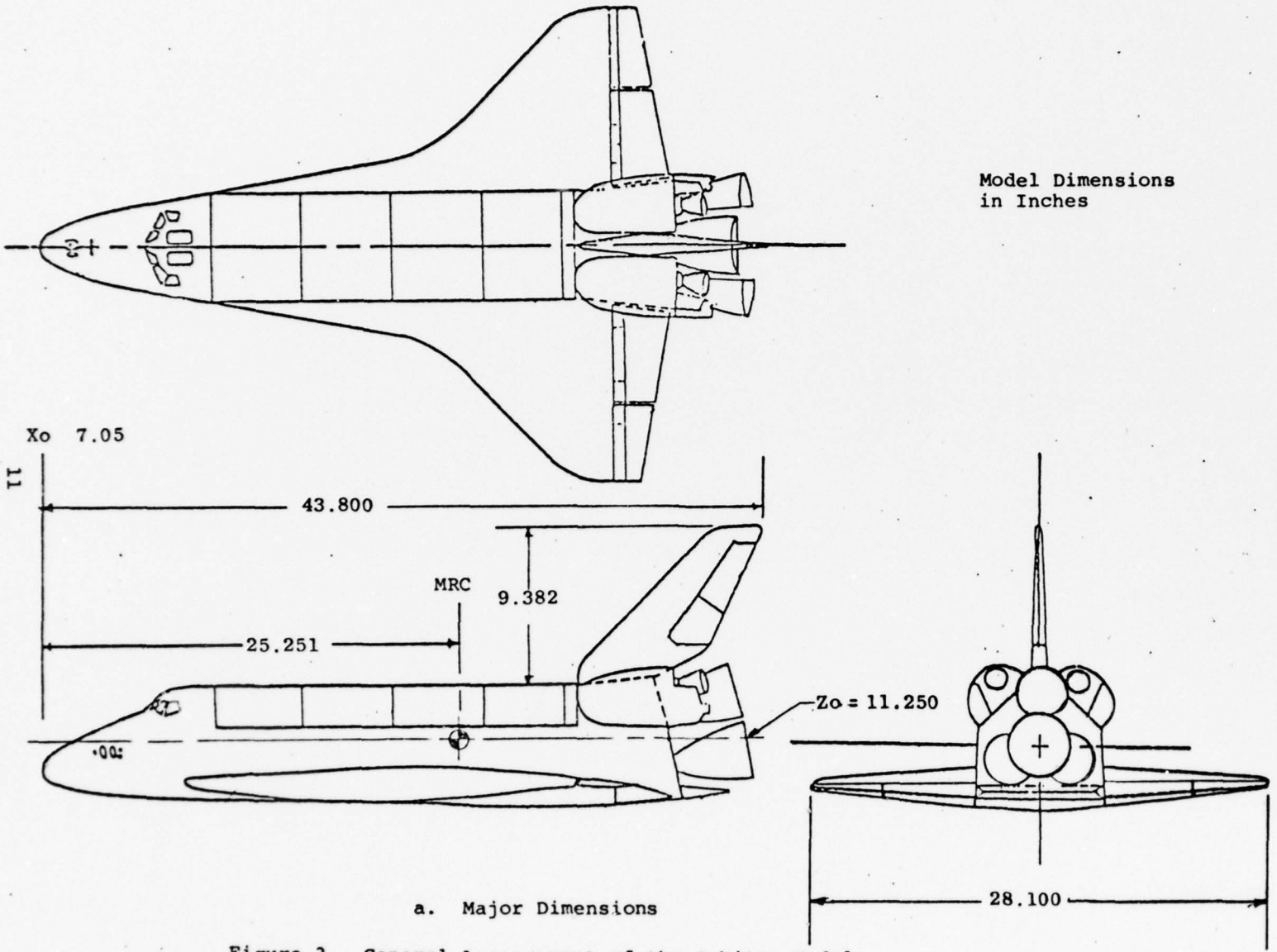

a. Major Dimensions

Figure 3. General Arrangement of the Orbiter Model

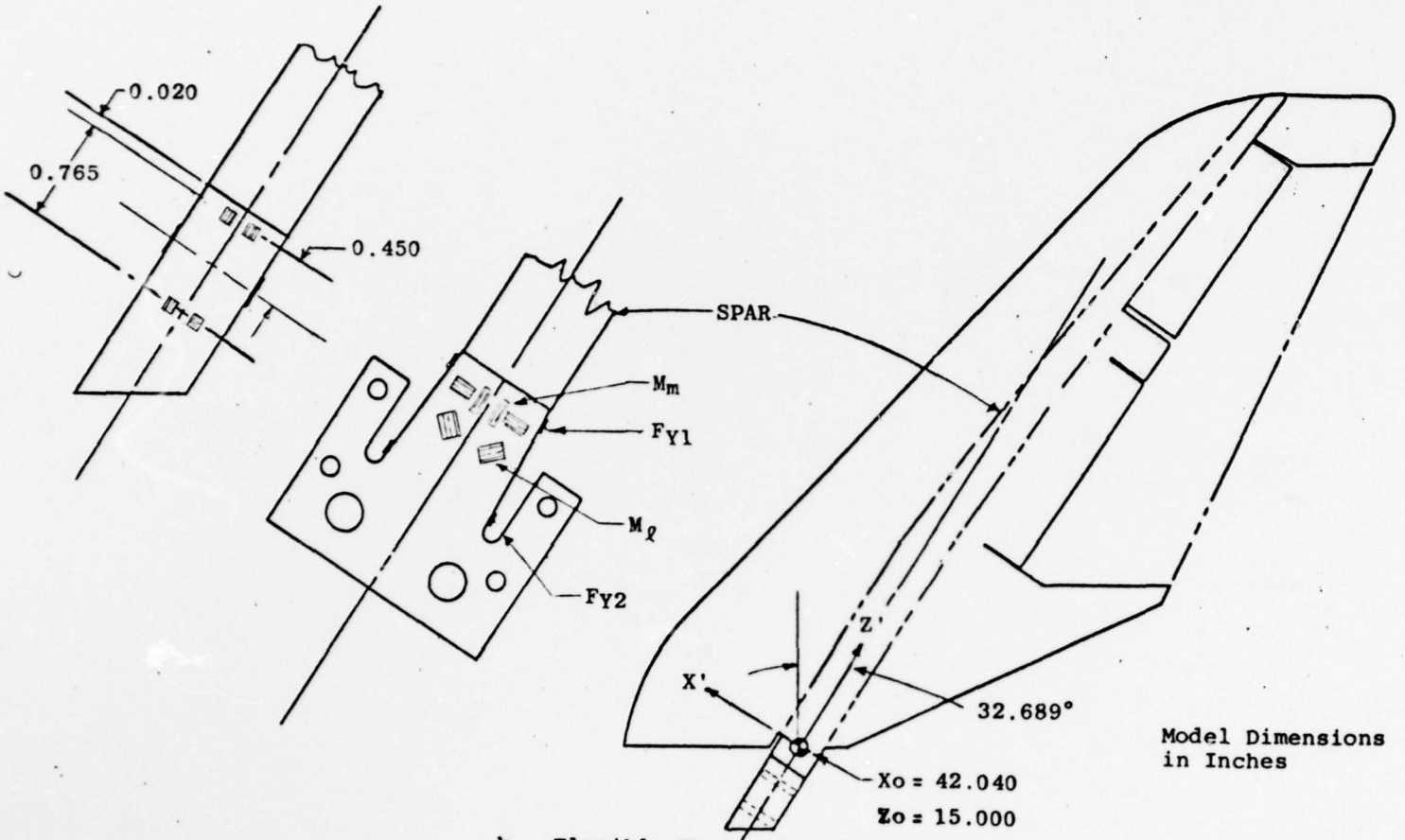

b. Flexible Vertical Tail

Figure 3. Concluded

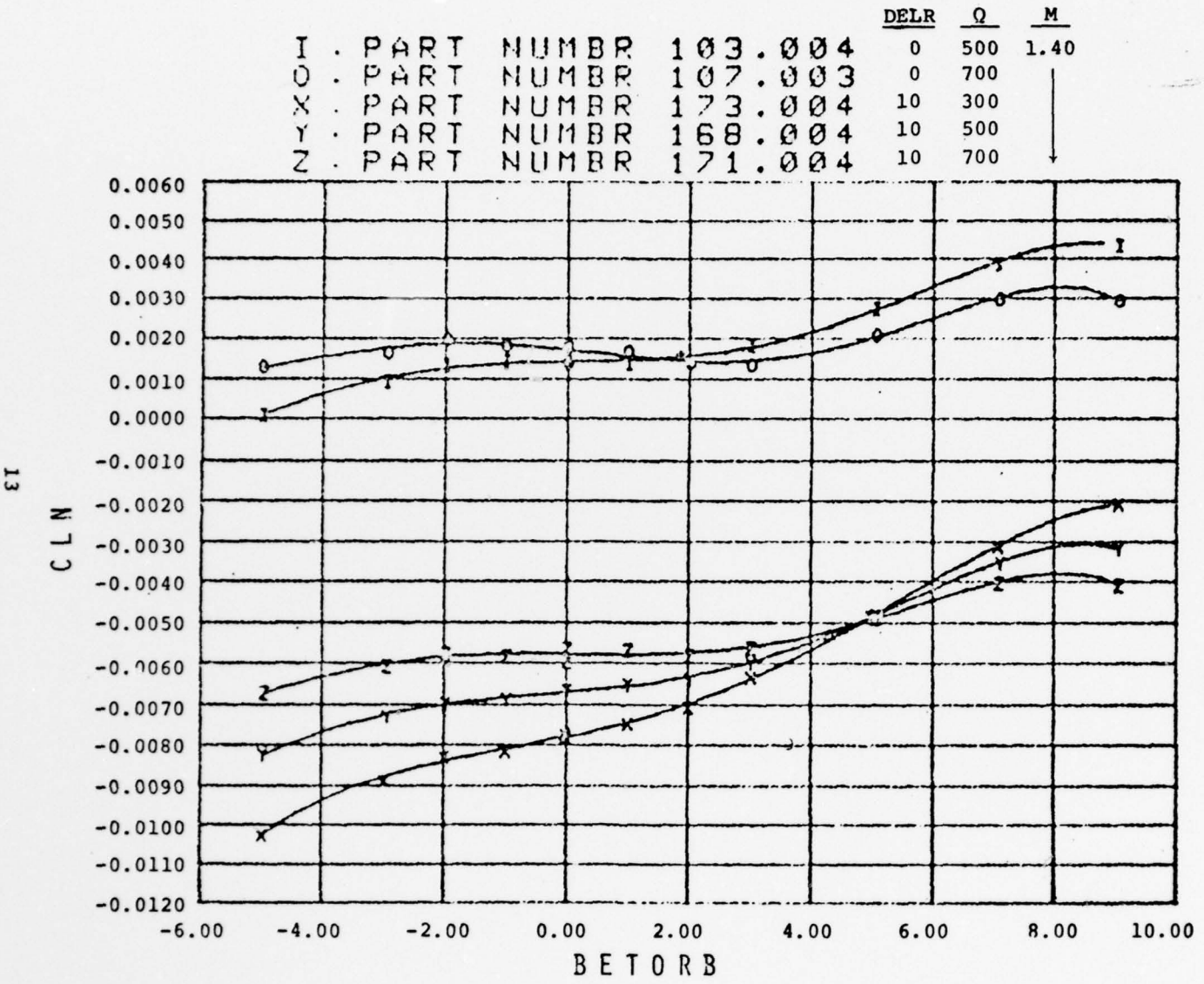

Figure 4. Typical Interactive Graphics Plot

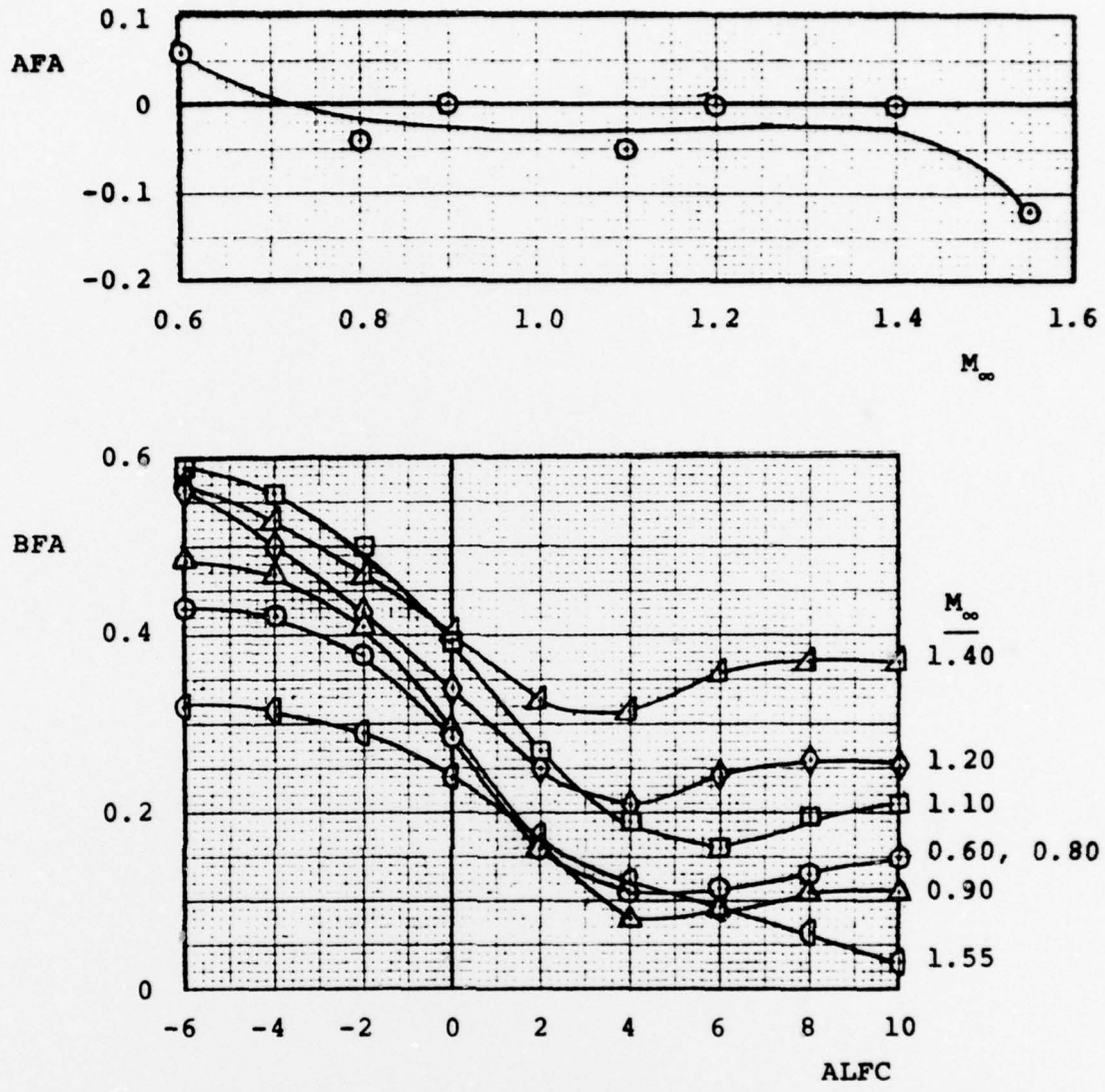

Figure 5. Pitch and Sideslip Flow Angularity

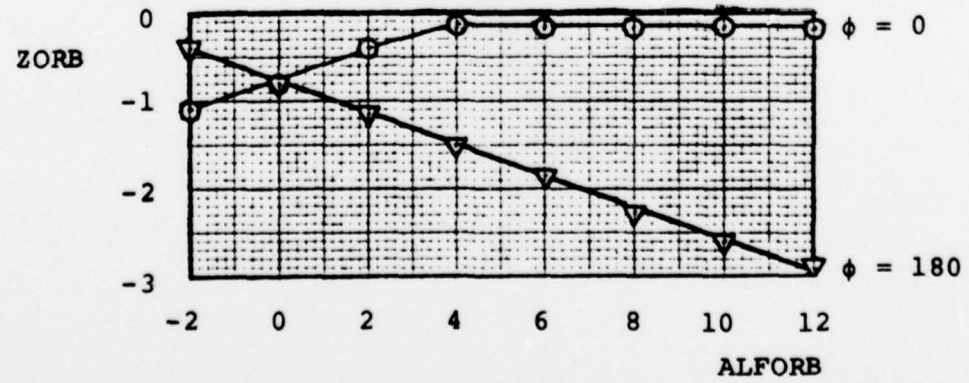

Figure 6. Vertical Location of Orbiter MRC with Angle of Attack Variation

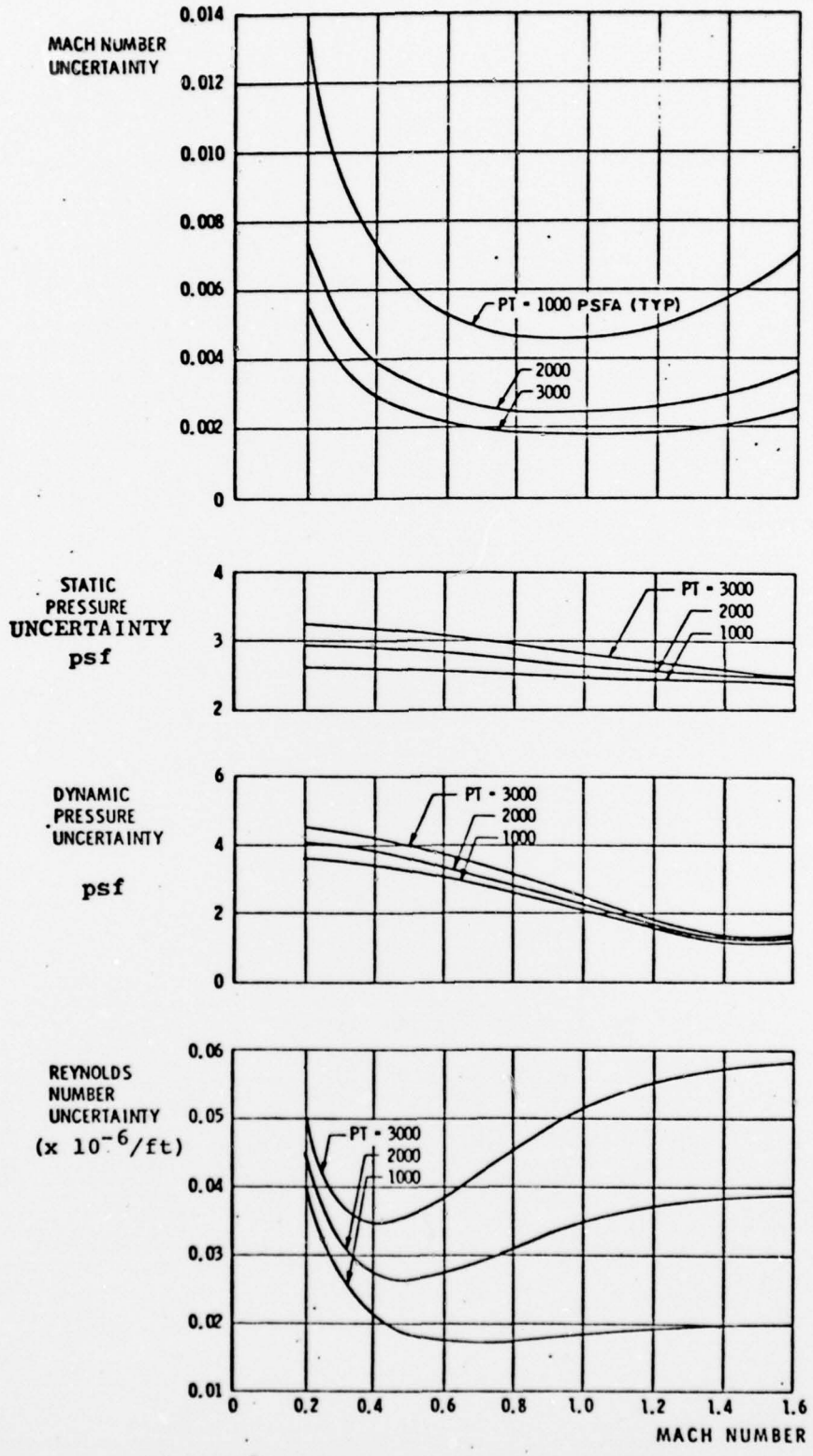

Figure 7. Estimated uncertainties in wind tunnel parameters.

Table 1

Model Attitude Schedules and Summary of Test Conditions

DELSB	DELR	M_∞	Q	Angle Schedules A	B	C	D	E	Flexible Tail
25	0	0.80	500	35*				36	
		0.90	300	43	42				
			500	46	44/45			47	
			750	50	49				
		1.10	300	73	71	72		70	
			500	59	57	58		55	
			700	62	74	61		60	
		1.20	300	81	80	79	82	76	
			500	88	86	87	89	85	
			700	96	93/94	95	97	92	
		1.40	300	114	112	113		111	
			500	105	103	104		102	
			700	110	107	108		109	
		1.55	300	125	124				
			500	117	116		118	115	
			700	122	121		123		

Note:

Schedule	Nominal Angles
A	α = -2, 0, 2, 4, 6, 8, 10, 12, 0 @ β = 0
B	β = -5, -3, -2, -1, 0, 1, 2, 3, 5, 7, 9, 0 @ α = 5
C	β = -5, -3, -2, -1, 0, 1, 2, 3, 5, 7, 9, 0 @ α = 10
D	α = -2, 0, 2, 4, 6, 8, 10, 12, 0 @ β = 2
E	β = -5, -3, -2, -1, 0, 1, 2, 3, 5, 7, 9, 0 @ α = 0

*PART Number

Table 1. Continued

DELSB	DELR	M_∞	Q	Angle Schedules A	B	C	D	E	Flexible Tail
25	10	0.90	300	129	128				
			500	131	130				
			700	134	133				
		1.10	300	144	143				
			500	140	139				
			700	142	141				
		1.20	300	152	151				
			500	147	146				
			700	150	149				
		1.40	300	174	173				
			500	170	168		169		
			700	172	171				
		1.55	300	159	158				
			500	156	155				
			700	154	153				
55	0	0.90	300	178	177				
			500	180	179				
			700	183	182				
		1.10	300	195	193	194		192	
			500	190	188	189		187	
			700	199	197	198		196	
		1.20	300	210	208	209	211	207	
			500	205/ 315	203/ 314	204/ 317	206/ 316	202/ 313	
			700	215	213	214	216	212	
		1.40	300	332	330	331		329	
			500	327	325	326		324	
			700	336	334	335		333	
		1.55	300	346	345				
			500	340	339				
			700	344	343				

Table 1. Continued

DELSB	DELR	M_∞	Q	Angle Schedules A	B	C	D	E	Flexible Tail
55	10	0.90	300	271	270				
			500	273	272				
			700	276	275				
		1.10	300	305	304				
			500	281	280				
			700	303	302				
		1.20	300	296	295				
			500	298	297				
			700	301	300				
		1.40	300	285	284				
			500	307	306				
			700	283	282				
		1.55	300	294	293				
			500	289	288				
			700	292	291				

Table 1. Concluded

			Angle Schedules			
DELSB	DELR	M_∞	Q	A	B	Rigid Tail
25	0	0.90	400	353	352	
↓	↓	1.10	↓	360	359	↓
		1.20		364	363	
		1.40		370	369	
↓	↓	1.55	↓	375	374	
25	10	0.90	400	378		
↓	↓	1.10	↓	384		
		1.20		386		
		1.40		391		
↓	↓	1.55	↓	396		
55	0	0.90	400	400	399	
↓	↓	1.10	↓	407	406	↓
		1.20		411	410	
		1.40		417	416	
	↓	1.55	↓	422	421	
	10	0.90	400	425		
	↓	1.10	↓	431		
		1.20		433		
		1.40		438		
↓	↓	1.55	↓	443		↓

Table 2

Summary of Test Conditions (Mach Number Sweep)

Tail	DELSB	DELR	Q	Mach Numbers																		
				0.60	0.65	0.70	0.75	0.80	0.85	0.90	0.95	1.00	1.05	1.10	1.15	1.20	1.25	1.30	1.35	1.40	1.45	1.50	1.55
Flexible	25	0	500	30*	31	32	33	34	40	41	51	52	53	54	75	90	98	99	100	101			119
	↓	10								132	135	136	137	138	145	148	165	166	167	162	161	160	157
	55	0								181	184	185	186	191	200	201	217	218	219	328	337	338	341
	↓	10	↓							274	277	278	279	246*	251*	299	259*	260*	261*	308	286	287	290
Rigid	25	0	400							354	355	356	357	358	361	362	365	366	367	368	371	372	373
	↓	10								379	380	381	382	383	385	387	388	389	390	392	393	394	395
	55	0								401	402	403	404	405	408	409	412	413	414	415	418	419	420
	↓	10	↓							426	427	428	429	430	432	434	435	436	437	439	440	441	442

Note:

Mach number sweep data were taken at two model attitudes at each Mach number:

$\alpha = 5$, $\beta = 0$, and $\alpha = 5$, $\beta = 5$ deg.

*Part Number

Table 3

Summary of Test Conditions

(Flow Angularity Diagnostic Runs)

Tail	DELSB	DELR	Q	Mach Numbers 0.60	0.80	0.90	1.10	1.20	1.40	1.55	Comments
Flexible	25	0	500		37*	48	56	91	106	120	β Variation @ ϕ = -90
Flexible	55	0	500		319	320	321	322	323	342	Roll Tare: α = 0, ϕ = -90 to 90
Rigid	25	0	400			462		467	470	473	Roll Tare: α = 0, ϕ = 0 to 180
↓	↓	↓	↓	457	460	461	465	466	471	472	ϕ = 0, α Variation
				458	459	463	464	468	469	474	ϕ = 180, Z = Z_{max}, α Variation
						476					ϕ = 180, Z = Z_{max} - 1 ft, α Variation
						477					ϕ = 180, Z = Z_{max} - 2 ft, α Variation

*Part Number

Table 4

Uncertainties of Aerodynamic Coefficients

M_∞	Q	ALFA/BETA	UCN	UCY	UCA	UCLL	UCLM	UCLN	UCYV	UCLLV	UCLNV
0.90	300	2/2	±0.0061	±0.0034	±0.0017	±0.0004	±0.0025	±0.0004	±0.0042	±0.0002	±0.0003
↓	↓	6/5	±0.0062	±0.0034	±0.0017	±0.0004	±0.0025	±0.0004	±0.0042	±0.0002	±0.0003
↓	↓	10/9	±0.0063	±0.0034	±0.0016	±0.0004	±0.0025	±0.0004	±0.0042	±0.0002	±0.0004
0.90	700	2/2	±0.0026	±0.0014	±0.0007	±0.0002	±0.0011	±0.0002	±0.0018	±0.0001	±0.0001
↓	↓	6/5	±0.0027	±0.0015	±0.0007	±0.0002	±0.0011	±0.0002	±0.0018	±0.0001	±0.0001
↓	↓	10/9	±0.0027	±0.0015	±0.0007	±0.0002	±0.0011	±0.0002	±0.0018	±0.0001	±0.0002
1.20	300	2/2	±0.0061	±0.0034	±0.0017	±0.0004	±0.0025	±0.0004	±0.0042	±0.0002	±0.0003
↓	↓	6/5	±0.0062	±0.0034	±0.0017	±0.0004	±0.0025	±0.0004	±0.0042	±0.0002	±0.0003
↓	↓	10/9	±0.0063	±0.0034	±0.0017	±0.0004	±0.0025	±0.0004	±0.0042	±0.0002	±0.0003
1.20	700	2/2	±0.0026	±0.0014	±0.0007	±0.0002	±0.0011	±0.0002	±0.0018	±0.0001	±0.0001
↓	↓	6/5	±0.0027	±0.0014	±0.0007	±0.0002	±0.0011	±0.0002	±0.0018	±0.0001	±0.0001
↓	↓	10/9	±0.0027	±0.0015	±0.0007	±0.0002	±0.0011	±0.0002	±0.0018	±0.0001	±0.0002
1.55	300	2/2	±0.0061	±0.0034	±0.0017	±0.0004	±0.0025	±0.0004	±0.0042	±0.0002	±0.0003
↓	↓	6/5	±0.0062	±0.0034	±0.0017	±0.0004	±0.0025	±0.0004	±0.0042	±0.0002	±0.0003
↓	↓	10/9	±0.0062	±0.0034	±0.0017	±0.0004	±0.0025	±0.0004	±0.0042	±0.0002	±0.0003
1.55	700	2/2	±0.0026	±0.0014	±0.0007	±0.0002	±0.0011	±0.0002	±0.0018	±0.0001	±0.0001
↓	↓	6/5	±0.0026	±0.0014	±0.0007	±0.0002	±0.0011	±0.0002	±0.0018	±0.0001	±0.0001
↓	↓	10/9	±0.0027	±0.0015	±0.0007	±0.0002	±0.0011	±0.0002	±0.0018	±0.0001	±0.0001

Uncertainties in longitudinal coefficients (C_N, C_A, and CLM) are presented for angles of attack of 2, 6, and 10 deg. Uncertainties in lateral-directional coefficients (CY, CLL, and CLN) and all vertical tail coefficients are presented for sideslip angles of 2, 5, and 9 deg.

Table 5

Summary Data Printout

DATE 18-AUG-78 PROJECT NO P411-34C

AND, INC.
AEDC DIVISION
A SVERDRUP CORPORATION COMPANY
PROPULSION WIND TUNNEL
ARNOLD AIR FORCE STATION, TENNESSEE

PROPULSION WIND TUNNEL
TRANSONIC 16T

BODY AXES COEFFICIENTS SUMMARY

PART 179 M= 0.900 PT= 1487.8 P= 880.1 Q= 498.5 RX10-6= 2.861

DEIL= 0.00 DECL= 0.00 DEIR= 0.233 DEOR= 0.186 DSB= 56.68 DR= -0.03

POINT	ALFORB	BETORB	CN	CY	CAF	CLM	CLL	CLN	CAB	CACAV	CAU	CA	CHEI	CHEO
3	5.08	-5.00	0.2190	0.1036	0.2069	0.0424	0.0083	-0.0127	-0.1075	-0.0002	0.0993	0.0995	0.0547	0.0290
5	4.95	-2.88	0.2109	0.0582	0.2032	0.0468	0.0056	-0.0061	-0.1037	-0.0003	0.0992	0.0995	0.0679	0.0331
7	4.98	-1.91	0.2093	0.0358	0.2038	0.0467	0.0034	-0.0035	-0.1042	-0.0005	0.0992	0.0996	0.0718	0.0362
9	4.99	-0.91	0.2174	0.0173	0.2069	0.0464	0.0020	-0.0017	-0.1067	-0.0007	0.0996	0.1003	0.0748	0.0329
11	4.95	0.08	0.2178	-0.0017	0.2110	0.0470	0.0008	0.0001	-0.1111	-0.0010	0.0998	0.1007	0.0771	0.0360
13	4.97	1.08	0.2086	-0.0224	0.2117	0.0484	-0.0002	0.0019	-0.1114	-0.0008	0.0995	0.1004	0.0793	0.0333
15	4.92	2.07	0.2058	-0.0436	0.2102	0.0482	-0.0014	0.0044	-0.1101	-0.0007	0.0994	0.1000	0.0811	0.0340
17	4.96	3.09	0.2116	-0.0658	0.2099	0.0466	-0.0026	0.0074	-0.1101	-0.0006	0.0992	0.0998	0.0826	0.0337
19	4.94	5.11	0.2127	-0.1118	0.2128	0.0431	-0.0052	0.0144	-0.1129	-0.0007	0.0993	0.0999	0.0849	0.0336
21	4.94	7.11	0.2127	-0.1586	0.2151	0.0414	-0.0087	0.0216	-0.1157	-0.0008	0.0987	0.0994	0.0860	0.0327
23	4.93	9.07	0.2103	-0.2032	0.2138	0.0374	-0.0128	0.0275	-0.1181	-0.0009	0.0948	0.0958	0.0848	0.0389
26	4.97	0.08	0.2134	-0.0011	0.2108	0.0475	0.0012	-0.0001	-0.1106	-0.0009	0.0993	0.1002	0.0762	0.0332

STABILITY AXES COEFFICIENT SUMMARY

POINT	ALFORB	BETORB	CL	CD	L/D	CLF	CDF	(L/D)F	XCP	EORB	CP10	CP13
3	5.08	-5.00	0.2094	0.1185	1.7670	0.1999	0.2255	0.8862	0.5787	-0.23	0.1205	0.3286
5	4.95	-2.88	0.2016	0.1173	1.7178	0.1926	0.2207	0.8729	0.5684	-0.12	0.1103	0.3366
7	4.98	-1.91	0.1998	0.1174	1.7023	0.1908	0.2212	0.8627	0.5678	-0.20	0.1046	0.3439
9	4.99	-0.91	0.2079	0.1188	1.7498	0.1986	0.2250	0.8824	0.5715	-0.26	0.0992	0.3408
11	4.95	0.08	0.2033	0.1187	1.7124	0.1937	0.2294	0.8446	0.5686	-0.11	0.0941	0.3440
13	4.97	1.08	0.1991	0.1181	1.6869	0.1895	0.2290	0.8275	0.5647	-0.08	0.0884	0.3440
15	4.92	2.07	0.1965	0.1173	1.6746	0.1870	0.2271	0.8237	0.5638	-0.15	0.0833	0.3453
17	4.96	3.09	0.2022	0.1177	1.7175	0.1927	0.2274	0.8471	0.5690	-0.16	0.0786	0.3429
19	4.94	5.11	0.2033	0.1179	1.7247	0.1936	0.2304	0.8402	0.5755	-0.17	0.0680	0.3361
21	4.94	7.11	0.2034	0.1174	1.7320	0.1934	0.2326	0.8312	0.5784	-0.18	0.0576	0.3283
23	4.93	9.07	0.2013	0.1135	1.7742	0.1912	0.2311	0.8273	0.5846	-0.20	0.0469	0.3036
26	4.97	0.08	0.2039	0.1183	1.7235	0.1943	0.2285	0.8507	0.5681	-0.07	0.0943	0.3409

VERTICAL TAIL COEFFICIENT SUMMARY

POINT	ALFORB	BETORB	CYV	CLNV	CLLV	XP	ZP	XCPV	ZCPV	EVT
3	5.08	-5.00	0.0484	-0.0213	0.0125	-0.31	4.40	1489.37	617.93	0.05
5	4.95	-2.88	0.0276	-0.0121	0.0069	-0.37	4.18	1487.09	610.50	0.27
7	4.98	-1.91	0.0174	-0.0075	0.0042	-0.40	3.90	1482.92	602.23	0.24
9	4.99	-0.91	0.0090	-0.0038	0.0020	-0.46	3.43	1475.81	587.86	0.23
11	4.95	0.08	0.0011	-0.0003	-0.0000	-0.61	4.89	1330.28	351.87	0.39
13	4.97	1.08	-0.0068	0.0033	-0.0021	-0.43	6.25	1525.96	667.61	0.40
15	4.92	2.07	-0.0159	0.0073	-0.0046	-0.37	5.37	1508.39	644.08	0.29
17	4.96	3.09	-0.0264	0.0120	-0.0074	-0.31	5.12	1502.32	637.96	0.23
19	4.94	5.11	-0.0466	0.0210	-0.0130	-0.28	5.02	1499.47	635.76	0.10
21	4.94	7.11	-0.0669	0.0301	-0.0188	-0.22	5.07	1498.68	638.38	-0.01
23	4.93	9.07	-0.0855	0.0386	-0.0246	-0.13	5.22	1498.86	644.11	-0.11
26	4.97	0.08	0.0045	-0.0016	0.0005	-0.20	-0.40	1399.62	485.22	0.43

Table 6

Nomenclature for Summary Data Printout

A_b	Orbiter model base area, 0.3930 ft^2
ALFORB	Orbiter model angle of attack, deg
BETORB	Orbiter model angle of sideslip, deg
BREF	Orbiter reference wing span, 28.100 in.
CA	Axial-force coefficient corrected for cavity effects, body axes, CA = CAU-CAC
CAB	Base axial-force coefficient, body axes force/QS_w
CACAV	Cavity axial-force coefficient, body axes force/QS_w
CAF	Forebody axial-force coefficient, body axes CAF = CA-CAB
CAU	Measured axial-force coefficient, body axes force/QS_w
CD	Drag coefficient, stability axes, force/QS_w
CDF	Forebody drag coefficient, stability axes, force/QS_w
CE	Elevon reference chord, 2.721 in.
CHEI	Inboard elevon hinge moment coefficient, moment/Q(SE)(CE)
CHEO	Outboard elevon hinge moment coefficient, moment/Q(SE)(CE)
CL	Lift coefficient, stability axes, force/QS_w
CLF	Forebody lift coefficient, stability axes, moment/QS_w
CLL	Orbiter rolling moment coefficient, body axes, moment/QS_w(BREF)
CLLV	Vertical tail torsion (rolling) moment, body axes, moment/QS_w(BREF)

Table 6. Continued

CLM	Orbiter pitching-moment coefficient, body axes, moment/QS_w(LREF)
CLN	Orbiter yawing moment coefficient, body axes, moment/QS_w(BREF)
CLNV	Vertical tail bending (yawing) moment coefficient, body axes, moment/QS_w(BREF)
CN	Orbiter normal-force coefficient, body axes, force/QS_w
CP10,13	Pressure coefficient, (PL-P)/Q
CY	Orbiter side-force coefficient, body axes, force/QS_w
CYV	Vertical tail side-force coefficient, body axes, force/QS_w
DEIL	Inboard left elevon deflection, deg
DEOL	Outboard left elevon deflection, deg
DEIR	Inboard right elevon deflection, deg
DEOR	Outboard right elevon deflection, deg
DR	Rudder deflection, deg
DSB	Speedbrake deflection, deg
LB	Body length, 38.709 in.
LREF	Wing reference chord, 14.244 in.
L/D	Lift to drag ratio
(L/D)F	Forebody lift to forebody drag ratio
M	Free-stream Mach number
P	Free-stream static pressure, psfa
PART	Part number (a data subset containing variations of only one independent parameter)
PL	Model local pressure, psfa
POINT	Point number (a single record of all test parameters)

Table 6. Concluded

PT	Free-stream total pressure, psfa
Q	Free-stream dynamic pressure, psf
$Rx10^{-6}$	Unit Reynolds number, per foot
SE	Elevon reference area, 0.189 ft^2
SW	Wing reference area, 2.241 ft^2
XCP	Orbiter center-of-pressure location referenced to LB
XCPV	Vertical tail center-of-pressure longitudinal location in full-scale coordinates, in.
XP,ZP	Location of vertical tail side force relative to vertical tail span root centerline, in.
ZCPV	Vertical tail center-of-pressure vertical location in full-scale coordinates, in.
ZORB	Location of orbiter moment reference center relative to the tunnel centerline, positive above, ft
ZVT	Location of a reference point on the vertical tail surface relative to the tunnel centerline, positive above, ft